

Bulk Photoemission from Plasmonic Nanoparticles: Physical Models and Software Tools

R. Sh. Ikhsanov¹, A. V. Novitsky², I. E. Protsenko³, and A. V. Uskov^{3,4}

¹National Research University Higher School of Economics, Moscow, Russia

²Technical University of Denmark, Kgs. Lyngby, Denmark

³Lebedev Physical Institute, Moscow, Russia

⁴ITMO University, St. Petersburg, Russia

Abstract— The paper presents our analytical and numerical results of calculations of bulk photoemission from metal nanoparticles of various shapes and sizes, embedded into semiconductor matrix. Software tools for calculation of characteristics of the effect are also developed.

1. INTRODUCTION

Generation of hot electrons in metallic plasmonic nanoparticles (nanoantennas) with their subsequent emission to semiconductor matrix attracts growing interest of researchers due to its potential applications in photochemistry and photo-catalysis, light harvesting (solar cells, nanophotodetectors and so on) and nano-optoelectronics, — in all areas of science and technology where the generation of hot photoelectrons and their utilization plays an important role [1]. In plasmonic nanoparticles two types of internal photoelectric effect may occur: the surface photoeffect [2] and the bulk photoeffect [3]. In this paper, we give results of our calculations of various characteristics (such as internal quantum efficiency, photoemission cross section and directionality ratio of the photocurrent) for the bulk photoelectric effect, obtained both analytically (for some simple shapes of nanoparticles and simple physical models) and numerically (for more complicated shapes and more complicated models). In addition to physical results, we present software tools to calculate characteristics of bulk photoelectric effect for nanoparticles of different shapes and sizes embedded into various semiconductor matrixes. The software is made by combining tools based upon Mathcad, Matlab and MNPBEM [5] software packages.

2. PHYSICAL MODEL OF THE BULK PHOTOEMISSION EFFECT

The bulk photoemission effect can be described as follows: (1) electron absorbs a photon inside metal, becoming hot, (2) then this hot electron moves toward the boundary between metal nanoparticle and surrounding semiconductor medium, being cooled due to collisions with cold electrons, and (3) finally overcomes the potential barrier on the boundary. Characteristics of the photoelectron emission are noticeably affected by plasmonic nanoantenna effect, which leads to strong enhancement of the field inside the metal nanoparticle and corresponding enhancement of generation of hot electrons inside the nanoparticle, and by the electron cooling when hot electron propagates in the nanoparticle. Both two effects strongly depend on size and shape of the nanoparticle. Although the cooling of hot electrons can be accurately described by Monte Carlo method, it is computationally very demanding. Instead we use the effective and simple model suggested in Ref. [4] for the first time. This model allows us to obtain not only the numerical results, but also achieve a deeper physical insight [3].

For a quantitative characterization of the photoemission from metallic nanoparticles, in which the electric field of the light wave is homogeneous (nanospheres and nanospheroids), we use the Internal Quantum Efficiency (IQE) η_i , which is, in fact, the probability for hot electron to leave nanoparticle, averaged over a nanoparticle volume [3]:

$$\eta_i = \frac{1}{V_n} \int_{V_n} \eta_i^{local}(\mathbf{r}) d^3r. \quad (1)$$

In this formula local IQE η_i^{local} is

$$\eta_i^{local}(\mathbf{r}) = \int_{V_k} P_{em}(\mathbf{r}, \mathbf{k}) \rho(k) d^3k / \int_{V_k} \rho_k(k) d^3k, \quad (2)$$

where $V_k = 4\pi(k_{\hbar\omega}^3 - k_F^3)/3$ is the volume of the phase layer ($k_F < k < k_{\hbar\omega}$) over Fermi surface of the metal; $\hbar k_F = \sqrt{2mE_F}$, $\hbar k_{\hbar\omega} = \sqrt{2m(E_F + \hbar\omega)}$, $\hbar\omega$ is the energy of the incident photon, k_F and E_F is Fermi wave vector and Fermi energy correspondingly; ρ_k is the effective electron density in the k -space; $P_{em}(\mathbf{r}, \mathbf{k})$ is probability that the photoelectron that is generated in the nanoparticle point \mathbf{r} with wave vector \mathbf{k} lives the nanoparticle. The probability P_{em} can be written as [3, 4]

$$P_{em}(\mathbf{r}, \mathbf{k}) = D(E(k), \alpha(\mathbf{r}, \mathbf{e}_k)) \times \exp(-L(\mathbf{r}, \mathbf{e}_k)/l_e), \quad (3)$$

where D is the coefficient of transmission of hot electron over the potential barrier at the interface between the nanoparticle and the semiconductor matrix; α is the angle of incidence of photoelectrons at the interface; $\mathbf{e}_k = \mathbf{k}/|\mathbf{k}|$ is the unit vector, co-directional with the vector \mathbf{k} ; $E(k)$ is the energy of photoelectron with wave number k (we use the simplest dispersion law $E(k) = \hbar^2 k^2/2m$); L is the distance along a straight line from the point of generation of a photoelectron to the boundary; l_e is the mean free path of electron. In calculation of D we use the model of a rectangular potential step, that takes into account difference in the masses of electron in metal (m) and semiconductor (m^*) [3].

For nanoparticles with non-uniform field distribution inside its volume, we calculate the photoemission cross-section (calculations of electric field distribution inside the nanoparticles are carried out for the incident linearly polarized light) as

$$\sigma_{pe}(\lambda) = \frac{2\pi}{\lambda} \frac{\varepsilon''_{met}}{n_{sem}} \int_{V_n} \eta_i^{local}(\mathbf{r}) E_i^2(\mathbf{r}) d^3r, \quad (4)$$

where n_{sem} is the refractive index of the semiconductor matrix (real number), ε''_{met} is the imaginary part of the nanoparticle's metal permittivity; $E_i(\mathbf{r})$ is the square of electric field in the nanoparticle (the electric field in the incident plane wave is assumed to be unit).

In order to characterize the directionality of the photoemission from nanoparticle we use the directionality ratio ρ , introduced in [6]:

$$\rho = \oint_S j_z(\mathbf{r}) dS / \oint_S \mathbf{j}(\mathbf{r}) \cdot d\mathbf{S}, \quad (5)$$

where j_z is the projection of the photoemission current density on the z-axis along the cone from the base with larger radius to the base with less one. Correspondingly, if $\rho > 0$, the net photocurrent from nanoparticle occurs in the direction of "sharp" end of the cone. The integration is carried out over the outer surface of the nanoparticle. Photoemission current density component that is normal to the surface of the nanoparticle at the point \mathbf{r}_0 is calculated with the formula

$$\begin{aligned} j_n(\mathbf{r}_0) \propto & \int_{V_k} \int_{V_n} \frac{\rho(k) E_i^2(\mathbf{r})}{4\pi L^2(\mathbf{r}, \mathbf{r}_0)} \times \exp\left(-\frac{L(\mathbf{r}, \mathbf{r}_0)}{l_e}\right) \times D(E(k), \alpha(\mathbf{r}, \mathbf{r}_0)) \\ & \times \cos(\alpha(\mathbf{r}, \mathbf{r}_0)) d^3r d^3k / \int_{V_k} \rho_k(k) d^3k, \end{aligned} \quad (6)$$

where \mathbf{r} is a point of generation of the photoelectron; $\alpha(\mathbf{r}, \mathbf{r}_0)$ is the angle of incidence of the photoelectron at the interface; $L(\mathbf{r}, \mathbf{r}_0)$ is the distance along a straight line from the point of generation of the photoelectron \mathbf{r} to the point at the boundary \mathbf{r}_0 .

Truncated cone is characterized by the conicity parameter defined in [6] as $\varsigma = 1 - R_1/R_2$, where R_1 is radius of the smaller cone base (in this work ς is also the ratio of the spheroid semi-axes).

3. SOFTWARE TOOLS AND THE MODEL PARAMETERS

The software, which we used in numerical calculations, was tools based upon Mathcad, Matlab and MNPBEM [5] software packages. With help of MNPBEM software package, running as a toolbox of MATLAB, electric field distribution in the nanoparticles (term $E_i^2(\mathbf{r})$ in formulae (4) and (6)) and the absorption cross section are calculated. Then square of electric field spatial distribution is passed as a data file to Mathcad-based software package that numerically calculates integrals for the different properties of the nanoparticles (such as internal quantum efficiency, photoemission cross section and directionality parameter). Below we provide the full set of the model parameters.

- E_F is the Fermi level of the metal;
- W is the work function of escape from the metal into the semiconductor;
- l_e is the hot-electron cooling length;
- m/m^* is the ratio of the effective masses of an electron in the metal (m) and in the semiconductor matrix (m^*);
- n_{matr} is semiconductor matrix refractive index;
- $\varepsilon_{met}(\lambda)$ is nanoparticle's metal permittivity;
- a and b are semiaxes of the spheroid;
- R_1, R_2, H are the bases radiuses and height of the truncated cone respectively.

The parameters with fixed values are presented in Table 1.

Table 1: Model parameters with fixed values.

E_F , eV	W , eV	l_e , nm	R_2 , nm	H , nm	n_{matr}	$\varepsilon_{met}(\lambda)$
5.51	0.8	41	20	40	3.6	<i>MNPBEM data base</i>

4. RESULTS OF CALCULATIONS

We have calculated mentioned above characteristics of the photoelectron emission for various shapes and sizes of nanoparticles, embedded into semiconductor matrix. Figure 1 shows IQE, denoted as η_i , for gold spheroidal nanoparticle embedded into homogeneous semiconductor medium as a function of the aspect ratio ζ (ratio of semiaxes a and b of the spheroid — see inset in Figure 1).

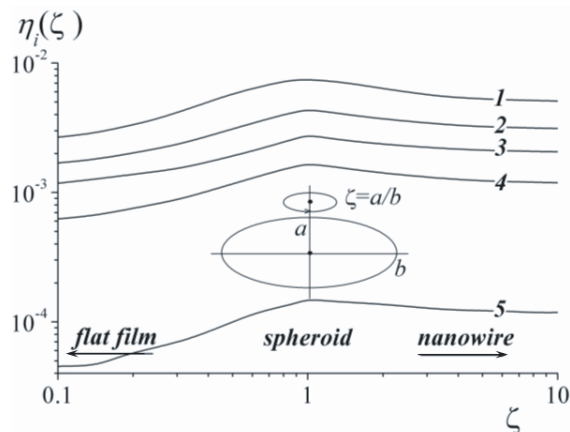


Figure 1: IQE for spheroidal nanoparticle as a function of the aspect ratio ζ . The vacuum wavelength of light, illuminating the nanostructure, is 1000 nm.

Aspect ratio $\zeta = 1$ corresponds to the sphere of diameter 50 nm, whereas $\zeta \rightarrow \infty$ does to the flat film of thickness 50 nm, and $\zeta \rightarrow +\infty$ corresponds to the nanowire of diameter 50 nm. Calculations are performed for gold nanostructure and GaAs semiconductor matrix [3]: For the illustration of the role of the electron cooling we present curves 1 and 3 with $l_e = \infty$ and $l_e = 20$ nm correspondingly (other curves were calculated with $l_e = 41$ nm). For the illustration of the influence of the difference of electron masses to IQE we calculated curve 4 with $m/ma^* = 2$ and curve 5 with $m/m^* = 10$ (curves 1–3 were calculated with $m/m^* = 1$). As one can see from Figure 1, the IQE ratios rates approximately as 3 : 2 : 1 for a sphere, cylinder and two-sided flat film with the same characteristic dimensions, placed in the homogeneous medium. This result just slightly (with an accuracy of 20%) depends on parameters of the model.

Figure 2 shows spectra of the absorption and photoemission cross-sections for a gold nanoparticle, having shape of truncated cone and embedded into GaAs matrix. The cross-sections were calculated for various values of the conicity parameter ς . A plane wave with linear polarisation, propagating along the axis of the cone, impinges on base of the nanoparticle with the radius R_1 —

see inset in Figure 2(a). In calculations we changed the radius R_1 , but other parameters of nanoparticle were fixed. Figure 2(a) shows evolution of the absorption cross-section of truncated cone with increasing of conicity parameter. Figure 2(b) demonstrates quite good correlation between behavior of the absorption and photoemission cross-sections, although the correlation deteriorates with increasing of ζ .

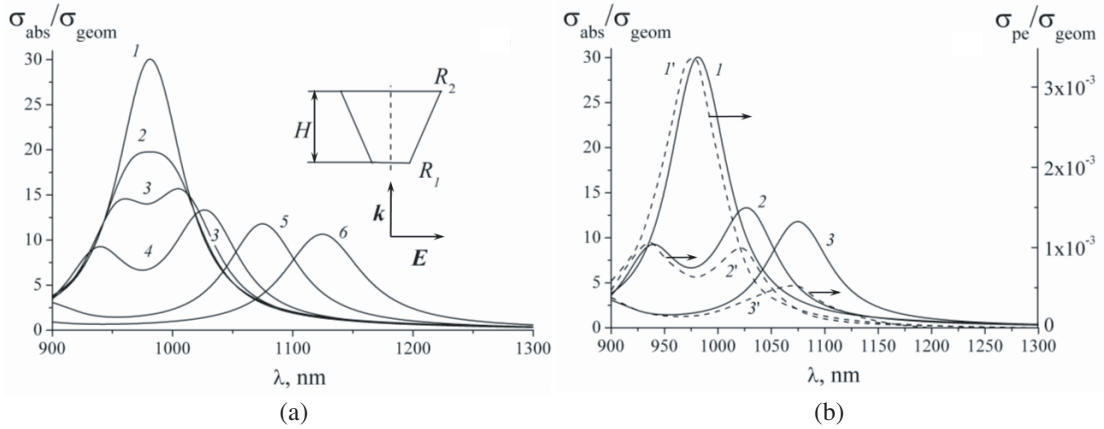


Figure 2: Spectra of the absorption σ_{abs} and photoemission σ_{pe} cross-sections for a nanoparticle with shape of truncated cone for various values of the conicity parameter ζ : (a) the absorption cross-section σ_{abs} for the conicity parameter $\zeta = 0$ (curve 1), 0.1 (2), 0.15 (3), 0.25 (4), 0.5 (5), 0.75 (6); (b) the absorption σ_{abs} (solid) and photoemission σ_{pe} (dashed) cross-sections for the conicity parameter $\zeta = 0$ (curve 1), 0.25 (3), 0.5 (3). $m/m^* = 15$; $\sigma_{geom} = \pi R_2^2$ is the geometrical cross-section of the nanoparticle.

The directionality parameter ρ in Eq. (5) can be nonzero due to the following factors: 1) anisotropic photoelectron release probability (multiplier $\exp(-L(\mathbf{r}, \mathbf{r}_0)/l_e) \times D(E(k), \alpha(\mathbf{r}, \mathbf{r}_0))$ in formula (6) — the probability that a photoelectron, which has absorbed a photon, experiences photoemission); 2) inhomogeneous distribution of the electric field inside the nanoparticle (multiplier $E_i^2(\mathbf{r})$ in formula (6)) and, correspondingly, inhomogeneous distribution of hot electron generation inside the nanoparticle. Figure 3(a) shows the influence of the first factor on the directionality ratio: we assume homogeneous field in the nanoparticle ($E_i^2(\mathbf{r}) = 1$ in formula (6)). Curves in this figure are calculated for various values for the ration m/m^* . Note that dependence on incident light wavelength is quite weak. As can be seen from the figure, the dependence $\rho(\zeta)$ for small ζ is linear, and the proportionality coefficient increases with increasing m/m^* .

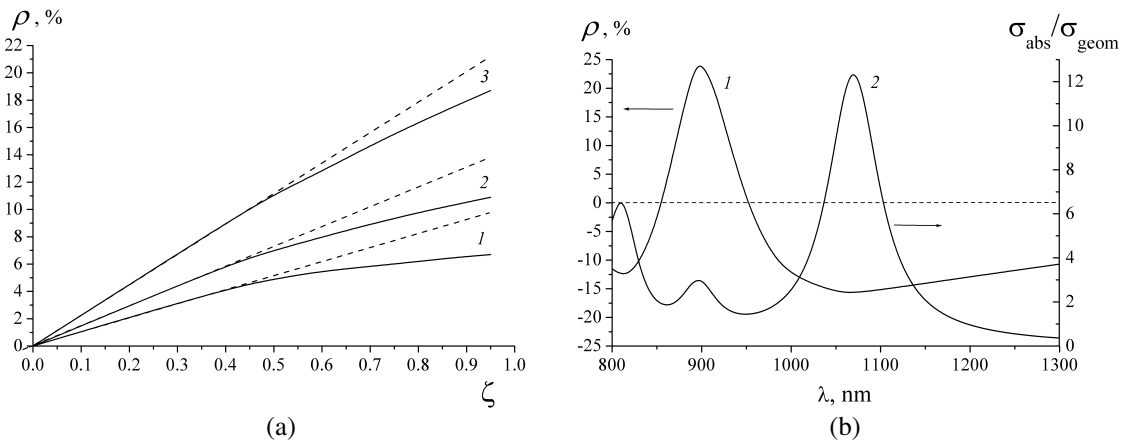


Figure 3: The directionality ratio ρ for nanoparticle with truncated cone shape: (a) homogeneous field distribution and anisotropic photoelectron release probability at various m/m^* ($\lambda = 1070$ nm): 1 (curve 1), 5 (2), 15 (3) (dashed curves show deviation of $\rho(\zeta)$ dependence from linear one); (b) inhomogeneous field distribution and isotropic photoelectron release probability at $\zeta = 0.5$: curve 1 — the directionality ratio spectrum, curve 2 — absorbance cross section spectrum.

Figure 3(b) shows the influence of the second factor on the directionality ratio: for the case of isotropic photoelectron release probability ($l_e = \infty$ and $D = 1$ in formula (6)) and inhomogeneous field distribution in the nanoparticle, $\rho(\zeta)$ dependence for $\zeta = 0.5$ is shown. As can be seen from the figure, the sign of the effect depends on the wavelength of incident light. This is due to the fact that the different plasmonic modes have different spatial distributions of electric field strength: for some modes the electric field is concentrated at the “sharp” base of the cone, while for the others — at the “obtuse” one. Curve 2 shows that sign of ρ changes during the transition from one mode to another.

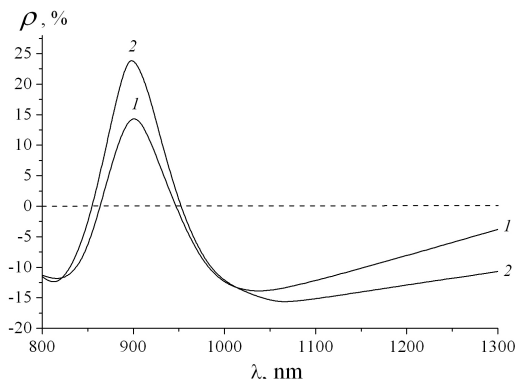


Figure 4: Spectrum of the directionality parameter ρ for nanoparticle with truncated cone form ($\zeta = 0.5$) for the general case of inhomogeneous field distribution and anisotropic photoelectron release probability at $m/m^* = 1$ (curve 1); curve (2) shows the directionality ρ calculated for inhomogeneous field distribution and isotropic photoelectron release probability.

Spectrum of the directionality ratio ρ , calculated with taking into account both factors, is shown in Figure 4. As can be seen from this figure, the directionality ratio spectrum, calculated with taking into account both factors, is well correlated with curve, calculated for the case, when factor (2) works alone, namely, when inhomogeneous distribution of the electric field in the nanoparticle is assumed. Thus, effect of inhomogeneous field distribution in the nanoparticle is dominating in realization of photogalvanic effect with bulk electron photoemission from asymmetric nanoparticles.

5. SOFTWARE TOOLS

The software, which we used in numerical calculations, was tools based upon Mathcad, Matlab and MNPBEM [5] software packages. With help of MNPBEM software package, running as a toolbox of MATLAB, electric field distribution in the nanoparticles and the absorption cross section are calculated. Integrals for the different properties of the nanoparticles (such as internal quantum efficiency, photoemission cross section and directionality parameter) are calculated by Mathcad software package.

6. CONCLUSION

We have developed broad software platform to calculate numerically characteristics (such as internal quantum efficiency, absorption and photoemission cross sections, anisotropy coefficient) of bulk electron photoemission from nanoantennas of various shapes and sizes, surrounded by various media. Also we have obtained analytical results for IQE of nanosphere, nanowire and thin film. Our results show that the bulk photoemission serves as efficient source of hot electrons for application in various areas of science and technology.

We have shown that electron cooling and the difference in effective electron masses in metal and semiconductor (by up to ~ 15 times for Au-GaAs pair) substantially influence the photoemission characteristics.

We have shown that the photoemission cross section of a nanoparticle of the truncated cone form is well correlated with its absorption cross section, especially near the plasmon resonance wavelength.

We have shown that the bulk photoemission can lead to the photogalvanic effect. similarly to the surface photoelectric effect [6]. Sign and magnitude of the directionality ratio, which characterizes this effect, depends on the wavelength of light (more precisely on field oscillations mode).

ACKNOWLEDGMENT

The work of A. U. was financially supported in part by the Government of the Russian Federation (Grant 074-U01) through the ITMO Visiting Professorship program. The authors acknowledge the COST Action MP1403 “Nanoscale Quantum Optics” for support.

REFERENCES

1. Brongersma, M. L., N. J. Halas, and P. Nordlander, “Plasmon-induced hot carrier science and technology,” *Nature Nanotechnology*, Vol. 10, No. 1, 25–34, 2015.
2. Uskov, A. V., I. E. Protsenko, R. Sh. Ikhsanov, et al., “Internal photoemission from plasmonic nanoparticles: comparison between surface and volume photoelectric effects,” *Nanoscale*, Vol. 6, 4716–4727, 2014.
3. Ikhsanov, R. Sh., V. E. Babicheva, I. E. Protsenko, A. V. Uskov, and M. E. Guzhva, “Bulk photoemission from metal films and nanoparticles,” *Quantum Electronics*, Vol. 45, 50–58, 2015.
4. Chen, Q. Y. and C. W. Bates, “Geometrical factors in enhanced photoyield from small metal particles,” *Phys. Rev. Lett.*, Vol. 57, No. 21, 2737–2740, 1986.
5. Hohenester, U. and A. Trügler, “MNPBEM — A Matlab toolbox for the simulation of plasmonic nanoparticles,” *Comp. Phys. Commun.*, No. 183, 370, 2012.
6. Zhukovsky, S. V., V. E. Babicheva, A. B. Evlyukhin, et al., “Giant photogalvanic effect in noncentrosymmetric plasmonic nanoparticles,” *Phys. Rev. X*, No. 4, 031038, 2014.